

Proceedings of the 17th Czech and Slovak Conference on Magnetism, Košice, Slovakia, June 3–7, 2019

Quantitative Analysis of Magnetoferritin-Induced Relaxivity Enhancement in MRI

O. STRBAK^{a,*}, L. BALEJCIKOVA^b, M. MIHALIKOVA^c, P. KOPCANSKY^d AND D. DOBROTA^c^aBiomedical Center Martin, Jessenius Faculty of Medicine in Martin, Comenius University in Bratislava, Mala Hora 4, 036 01 Martin, Slovakia^bInstitute of Hydrology, Slovak Academy of Sciences, Dubravska cesta 9, 841 04 Bratislava, Slovakia^cDepartment of Medical Biochemistry, Jessenius Faculty of Medicine in Martin, Comenius University in Bratislava, Mala Hora 4, 036 01 Martin, Slovakia^dInstitute of Experimental Physics, Slovak Academy of Sciences, Watsonova 47, 040 01 Kosice, Slovakia

Various disorders, including neurodegenerative diseases, are associated with iron accumulation. Ferritin particles are believed to be a precursor of pathological iron core transformation and iron accumulation, forming so-called pathological ferritin. Magnetoferritin is currently considered as the most suitable model system of pathological ferritin. It is described as apoferritin containing a magnetite nanocrystal. The magnetic moment of magnetoferritin is significantly larger than the magnetic moment of native ferritin containing ferrihydrite crystal. Theoretically, the effect of magnetoferritin on longitudinal and transverse relaxivity should also be significantly higher. Therefore, we provide a quantitative analysis of the magnetoferritin-induced enhancement of longitudinal and transverse relaxivity. However, our results at 7 T MRI indicate that a transverse relaxation significantly prevails in magnetoferritin compared to native ferritin. Such a quantitative analysis is essential for developing the MRI methodology required for non-invasive diagnostics of pathological processes associated with iron accumulation.

DOI: [10.12693/APhysPolA.137.720](https://doi.org/10.12693/APhysPolA.137.720)

PACS/topics: ferritin, magnetoferritin, MRI, relaxivity, non-invasive diagnostics

1. Introduction

Biological iron is associated with a variety of pathological processes, particularly neuroinflammatory processes [1], and neurodegenerative diseases [2]. It is generally accepted that these pathological processes are associated with disrupted iron homeostasis that results in iron accumulation and the formation of aggregates in the form of nanosized iron oxide particles [2]. Ferritin has been proposed as the precursor of such accumulated iron [3]. It is formed by a protein envelope (12 nm) and a mineral core (2–7 nm) in the form of crystalline ferrihydrite [4]. The primary role of ferritin in the body is the elimination of toxic ferrous ions upon reaching their critical concentration for the organism and depositing them in the form of nontoxic ferric ions for later usage by the organism. In 2004, Quintana et al. utilized electron nanodiffusion and electron microscopy to show that the ferritin mineral nucleus of patients with Alzheimer's disease (referred to as "pathological" ferritin) is structurally different from native (physiological) ferritin [3]. In physiological ferritin, the mineral core consists mainly of hexagonal ferrihydrite, hematite, and a smaller phase of magnetite. In contrast, the core of pathological ferritin consists mainly of cubic structures, such as magnetite and wüstite, and to a lesser extent ferrihydrite, with the absence of hematite. These

conclusions have been confirmed by a recent study [5], where muon spin rotation was used to show that the ferritin particles have a crystalline phase with large magnetocrystalline anisotropy that is compatible with magnetite or maghemite. Pathological ferritin is thus better described by magnetoferritin, which is composed of apoferritin and an artificially added phase of magnetite or maghemite [6]. The magnetic moment of magnetoferritin is significantly larger than the magnetic moment of the native ferritin core, therefore a more than 200-fold increase in the longitudinal and transverse relaxation rates of magnetoferritin is expected [5]. Based on these theoretical expectations, we provide a quantitative analysis of the longitudinal and transverse relaxation rates, as well as the relaxivity, of magnetoferritin and native ferritin particles with a 7 T MRI system. These results should contribute to the development of an MRI methodology required for non-invasive diagnostics of pathological processes associated with iron accumulation (neurodegenerative disorders, neuroinflammation, cirrhosis, lung and heart diseases).

2. Materials and methods

Magnetoferritin was prepared by the incorporation of ferrous ions into the empty protein shell of native apoferritin by the synthesis method described in [7]. Three different loading factors, representing the average number of iron atoms per apoferritin, were prepared: $LF_A = 553$, $LF_B = 733$, and $LF_C = 872$. The loading factor of native ferritin (NF) was determined as 884. Quantitative analysis of the loading factor was performed using a UV-vis

*corresponding author; e-mail: oliver.strbak@centrum.cz

spectrophotometer (SPECORD 40, Analytik Jena) at 2cc with a precision of $\approx 1\%$.

The MRI relaxivity measurements were performed using a 7 T BioSpec Bruker system. The concentration gradient of iron oxide (2.5×10^{-3} –0.02) mg/ml of ferrihydrite in ferritin, and magnetite in magnetoferritin) and two different MRI protocols were used for the determination of the longitudinal and transverse relaxation rates (R_1 and R_2) and relaxivity (r_1 and r_2):

- RARE — rapid acquisition with refocused echoes (T_1 mapping),
- MSME — multi-slice multi-echo (T_2 mapping).

The relaxation rate R_n is inverse to the relaxation time

$$R_n = \frac{1}{T_n}, \quad (n = 1, \text{ or } 2). \quad (1)$$

The relaxation times were determined by fitting the signal intensity values. The change in R_n is defined as the relaxivity of the magnetic particles:

$$r_n = \frac{R_n - R_n^0}{C} \quad (n = 1, \text{ or } 2), \quad (2)$$

where R_n^0 is the relaxation rate in the absence of iron oxide core, R_n represents the relaxation rate in the presence of iron oxide core, and C is the iron oxide concentration.

The Paravision Image Sequence Analysis tool (Bruker, Germany), and Matlab R2019a (Mathworks Inc., USA) were employed for data processing.

3. Results

Comparisons of the longitudinal and transverse relaxation rates of native ferritin and magnetoferritin are shown in Fig. 1a and b, respectively. The relaxation rates were calculated from Eq. (1), while the relaxation times were determined by fitting the signal intensity. For both relaxation rates, all the magnetoferritins with different loading factors are clearly distinguishable from the native ferritin. However, for the longitudinal relaxation rate R_1 (Fig. 1a), the difference is not so significant as the contrast in the transverse relaxation rate R_2 (Fig. 1b). Quantitatively, these differences are shown in Fig. 1c and 1d, as the ratio of magnetoferritin to native ferritin. While for the longitudinal relaxation rate R_1 , the range is from ≈ 1.1 to 1.8 in favor of magnetoferritin, for the transverse relaxation rate R_2 , it is already up to ≈ 7 –50 in account of magnetoferritin.

The longitudinal and transverse relaxivity of native ferritin and magnetoferritin are described in Figs. 2a and 2b. Similar to the relaxation rate changes, the longitudinal relaxivity (Fig. 2a) of magnetoferritin is only slightly higher ($r_1(\text{LFA}) = 2.17 \text{ mM}^{-1} \text{ s}^{-1}$, $r_1(\text{LFB}) = 1.5 \text{ mM}^{-1} \text{ s}^{-1}$, and $r_1(\text{LFC}) = 1.2 \text{ mM}^{-1} \text{ s}^{-1}$) in comparison with native ferritin, namely $r_1(\text{NF}) = 0.4 \text{ mM}^{-1} \text{ s}^{-1}$. In contrast, the transverse relaxivity (see Fig. 2b) of magnetoferritin ($r_2(\text{LFA}) = 320 \text{ mM}^{-1} \text{ s}^{-1}$, $r_2(\text{LFB}) = 527.7 \text{ mM}^{-1} \text{ s}^{-1}$ and $r_2(\text{LFC}) = 402.3 \text{ mM}^{-1} \text{ s}^{-1}$)

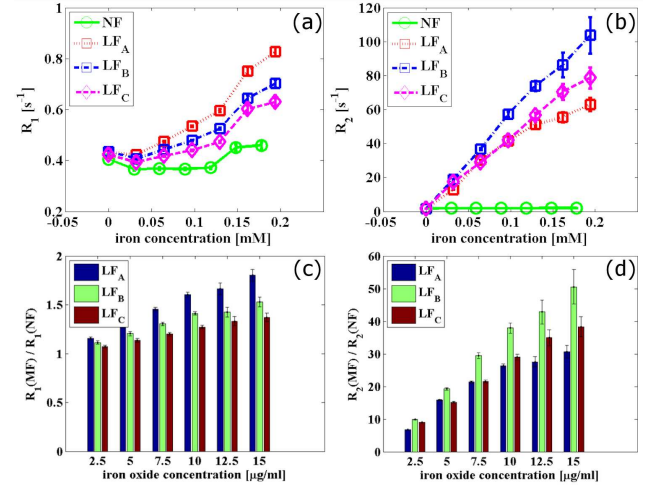


Fig. 1. Comparison of native ferritin and magnetoferritin: (a) longitudinal relaxation rate R_1 , (b) transverse relaxation rate R_2 . Ratio of magnetoferritin to native ferritin: (c) longitudinal relaxation rate R_1 , (d) transverse relaxation rate R_2 .

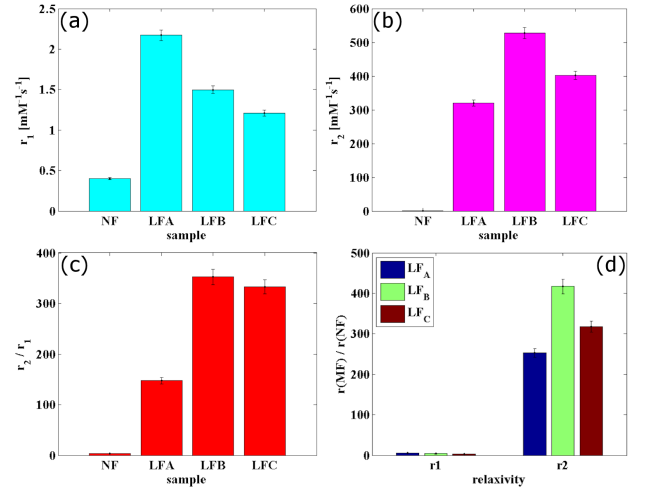


Fig. 2. Relaxivity comparison of native ferritin and magnetoferritin: (a) longitudinal relaxivity r_1 , (b) transverse relaxivity r_2 , (c) ratio of transverse and longitudinal relaxivity r_2/r_1 , (d) relaxivity ratio of magnetoferritin to native ferritin.

is significantly larger in comparison with native ferritin ($r_2(\text{NF}) = 1.27 \text{ mM}^{-1} \text{ s}^{-1}$). The ratio of transverse and longitudinal relaxivity (r_2/r_1) is high (Fig. 2c), proving the characteristics of magnetoferritin as a T_2 contrast agent [8]. The quantitative analysis of the magnetoferritin-induced relaxivity enhancement is displayed in Fig. 2d. The ratio of magnetoferritin and native ferritin is of the order of less than 10-times for longitudinal relaxivity ($\text{LFA} = 5.4$, $\text{LFB} = 3.7$, and $\text{LFC} = 3.0$), while for transverse relaxivity, it is of order of 100-times ($\text{LFA} = 252.9$, $\text{LFB} = 416.9$, and $\text{LFC} = 317.8$).

4. Discussion

Based on theoretical calculations, a more than 200 times larger effect of magnetite-like particles (magnetoferritin) is expected on R_1 and R_2 of the surrounding water protons compared to the effect of ferrihydrite-like particles (native ferritin) [9]. However, our results indicate the minimal effect of synthetically prepared magnetoferritin on R_1 at 7 T (Fig. 1a). Depending on the loading factor and iron oxide concentration, it is in the range of 1.1 to 1.8 times (Fig. 1c). In contrast, R_2 is significantly larger in magnetoferritin than in native ferritin (Fig. 1b). Quantitatively, it ranges from an almost 10 times enhancement to a ≈ 50 times enhancement (Fig. 1d). Although it is not the expected value, the comparison with [10] is very similar. At 7 T, they observed a 125-fold increase in the transverse relaxation rate of magnetoferritin in comparison with normal brain ferritin. However, the result was normalized for an iron concentration of 10 mM, which is still significantly more than our most concentrated sample (0.24 mM of iron). The r_1 and r_2 values naturally copy the values of the relaxation rates (Fig. 2a and 2b), indicating the prevailing transverse relaxation effect of magnetoferritin on surrounding water protons. This is also supported by the high r_2/r_1 ratio of magnetoferritin (from 147.3 to 352.2, 3.2 for native ferritin, Fig. 2c) that characterizes the efficiency of the paramagnetic molecule for contrast properties [7]. The observed transverse relaxivity of magnetoferritin is even larger compared to commercially used iron oxide contrast agents: Feridex, $r_2 = 120 \text{ mM}^{-1} \text{ s}^{-1}$; Resovist, $r_2 = 186 \text{ mM}^{-1} \text{ s}^{-1}$; Combidex, $r_2 = 65 \text{ mM}^{-1} \text{ s}^{-1}$ [7]. The ratio of magnetoferritin relaxivity to native ferritin relaxivity in Fig. 2d quantitatively proves the significant effect of transverse relaxation (252.9–416.9 times enhancement) in comparison with longitudinal relaxation (3.0–5.4 times enhancement).

5. Conclusions

We have quantified the effect of magnetoferritin nanoparticles on longitudinal and transverse relaxation rates and relaxivity in comparison with native ferritin. Our results show the prevailing effect of magnetoferritin particles on the transversal relaxation of surrounding water protons at 7 T. Such a quantitative analysis is required for the development of an MRI methodology for the non-invasive diagnostics of pathological processes associated with iron accumulation (neurodegenerative disorders, neuroinflammation, cirrhosis, lung and heart diseases).

Acknowledgments

This work was supported by the projects: Ministry of Health (2018/11-UKMT-7), VEGA (2/0016/17, 2/0044/20), APVV (APVV-015-0453), and Competence Center Martin (ITMS code: 26220220153).

References

- [1] T.C. Frank-Cannon, L.T. Alto, F.E. McAlpine, M.G. Tansey, *Mol. Neurodegener.* **16**, 47 (2009).
- [2] J. Hagemeyer, J.J.G. Geurts, R. Zivadinov, *Expert Rev. Neurother.* **12**, 1467 (2012).
- [3] C. Quintana, J.M. Cowley, C. Marhic, *J. Struct. Biol.* **147**, 166 (2004).
- [4] N.D. Chasteen, P.M. Harrison, *J. Struct. Biol.* **126**, 182 (1999).
- [5] L. Bossoni, L.G. Moursel, M. Bulk, et al., *J. Phys. Condens. Matter* **29**, 415801 (2017).
- [6] L. Xue, D. Deng, J. Sun, *Int. J. Mol. Sci.* **20**, 2426 (2019).
- [7] O. Strbak, L. Balejčiková, L. Baciak, J. Kovac, M. Masarova-Kozelova, A. Krafčík, D. Dobrota, P. Kopcansky, *J. Phys. D Appl. Phys.* **50**, 365401 (2017).
- [8] J. Estelrich, M.J. Sanchez-Martin, M.A. Busquets, *Int. J. Nanomed.* **10**, 1727 (2015).
- [9] A. Roch, R.N. Muller, P. Gillis, *J. Chem. Phys.* **110**, 5403 (1993).
- [10] Y. Gossuin, D. Hautot, R.N. Muller, Q. Pankhurst, J. Dobson, C. Morris, P. Gillis, J. Collingwood, *NMR Biomed.* **18**, 469 (2005).